Supplementary Figure 1

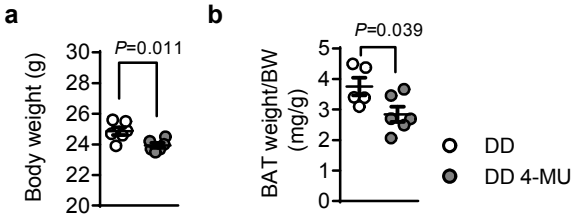

Supplementary Figure 1 4-MU decreases body weight and brown adipose tissue (BAT) mass independent of food intake. (**a**) Body weight (n = 6,6 mice) and (**b**) BAT weight normalized to body weight (BW; n = 5,6 mice) after one week of pair feeding C57BL6/J mice with diabetogenic diet (DD) or DD supplemented with 4-MU. Data are presented as means ± s.e.m., (**a**, **b**) two-tailed unpaired Student's *t*-test.

Supplementary Figure 2

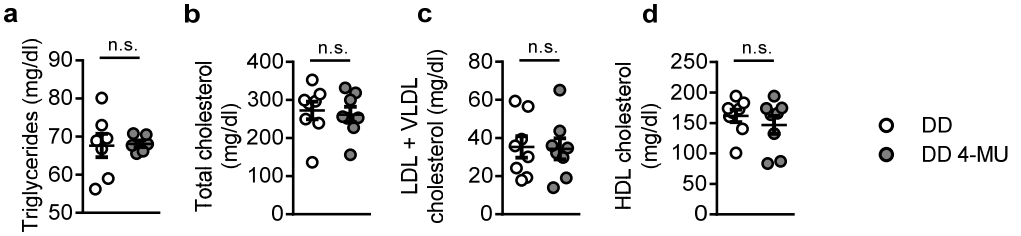

Supplementary Figure 2 No changes in plasma lipids after treatment with 4-MU. (**a**) Triglycerides (n = 7,6 biologically independent samples), (**b**), total cholesterol (n = 8,8 biologically independent samples), (**c**) low density lipoprotein (LDL) + very low density lipoprotein (VLDL) cholesterol (n = 8,8 biologically independent samples) and (**d**) high density lipoprotein (HDL) cholesterol (n = 8,8 biologically independent samples) concentrations in plasma of C57BL/6J mice after 22 weeks of feeding either DD or DD 4-MU. Data are presented as means ± s.e.m., (**a-d**) two-tailed unpaired Student's *t*-test. n.s.: not significant.

Supplementary Figure 3

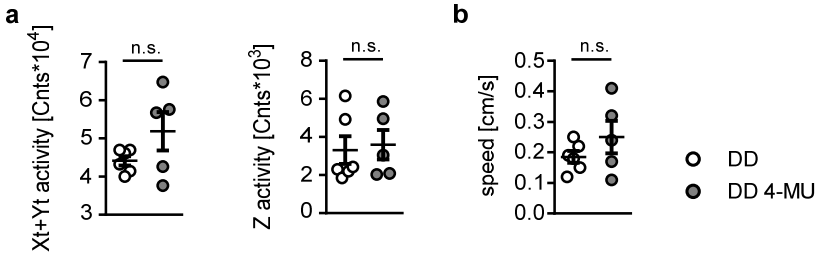

Supplementary Figure 3 4-MU treatment does not change locomotor activity in mice. After 5 weeks of feeding C57BL/6J mice with either diabetogenic diet (DD) or DD supplemented with 4-MU (DD 4-MU), their spontaneous locomotor activity was measured, revealing no changes in (**a**) the X, Y, or Z plane or in (**b**) speed; n = 6,5 mice. Data are presented as means ± s.e.m.. (**a**, **b**) Two-tailed unpaired Student's *t*-test. n.s.: not significant.

Supplementary Figure 4

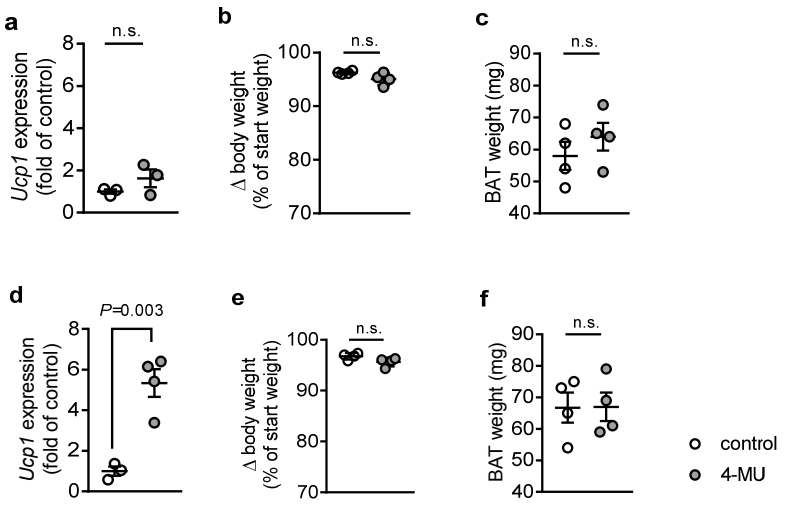

Supplementary Figure 4 Rapid upregulation of *Ucp1* mRNA expression independently from changes in body weight. Male, 8-week-old C57BL/6J mice were treated with 4-MU or respective placebo for 6 (**a-c**) or 9 hours (**d-f**) followed by analysis of *Ucp1* mRNA expression (**a**, **d**), changes in body weight during treatment (**d**, **e**) and BAT weight at time of harvest (**c**, **f**). Data are presented as means ± s.e.m.; n = 3,4 mice. (**a-f**) Two-tailed unpaired Student's *t*-test. n.s.: not significant.

Supplementary Figure 5

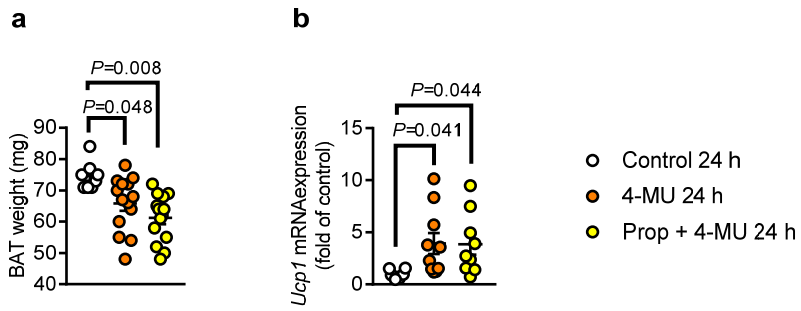

Supplementary Figure 5 No effects of propranolol on 4-MU-induced decrease in brown adipose tissue (BAT) weight and increase in *Ucp1* mRNA expression. Male, 8-week-old C57BL/6J mice were pretreated with propranolol (prop; 0.5 mg/day) for three days prior to application of 4-MU or respective vehicle control. (**a**) BAT weight after 24 hours of 4-MU treatment in the presence or absence of prop; n = 8,14,14 biologically independent samples, and (**b**) 4-MU- induced increase in *Ucp1* mRNA expression in presence or absence of propranolol; n = 6,10,9 biologically independent samples. Data are presented as means ± s.e.m.. (**a, b**) One-way ANOVA with post hoc Sidak`s multiple comparison test.

Supplementary Figure 6

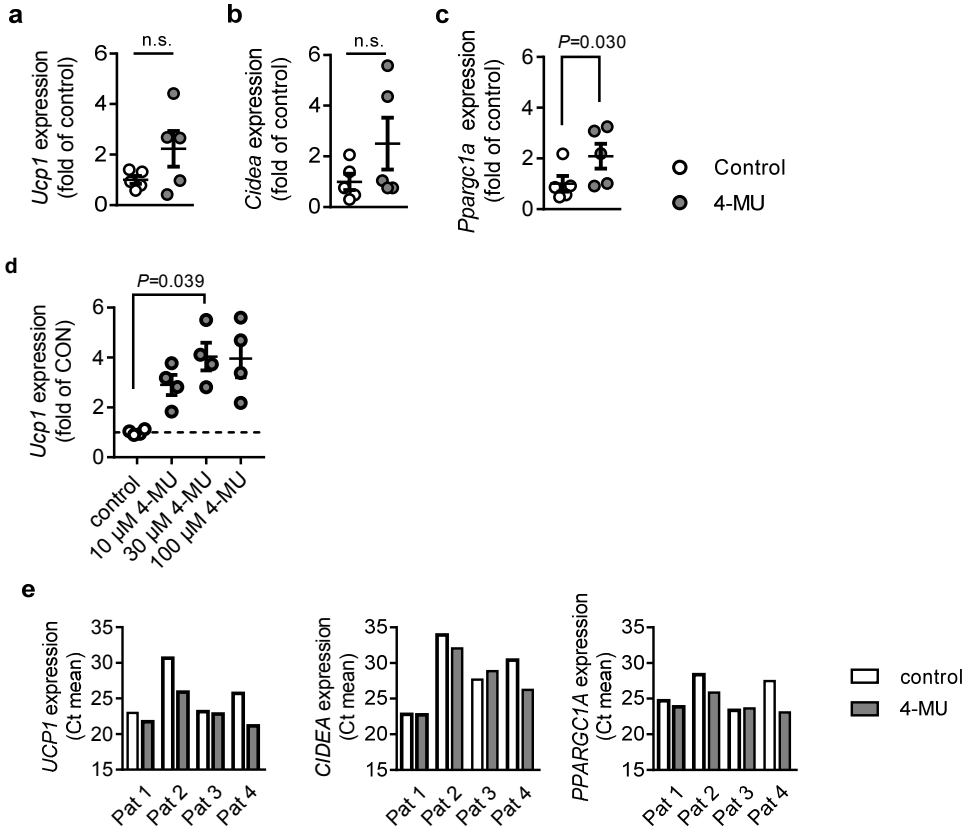

Supplementary Figure 6 4-MU increases brown adipose tissue (BAT) activation markers in murine differentiated brown adipocytes. (**a**) *Ucp1,* (**b**) *Cidea,* and (**c**) *Ppargc1a* mRNA expression in primary differentiated murine brown adipocytes after 24 h treatment with 4-MU (100 µM) or respective control as determined by qPCR, n = 5,5 biologically independent samples. (**d**) Undifferentiated T37i cells were treated with the indicated concentrations of 4-MU or respective control for 24 hours followed by determination of *Ucp1* mRNA by qPCR; n = 4 biologically independent samples. (**e**) *UCP1*, *CIDEA*, and *PPARGC1A* mRNA expression, as determined by qPCR, in human differentiated brown adipocytes isolated from 4 patients (Pat) and treated with 4-MU (100 µM) or respective vehicle (control) for 24 h. Data are presented as means ± s.e.m.. (**a, b**) Two-tailed Paired Student's *t*-test or (**c**) Mann-Whitney test, (**d**) one-way ANOVA with Sidak's multiple comparisons test. n.s.: not significant.

Supplementary Figure 7

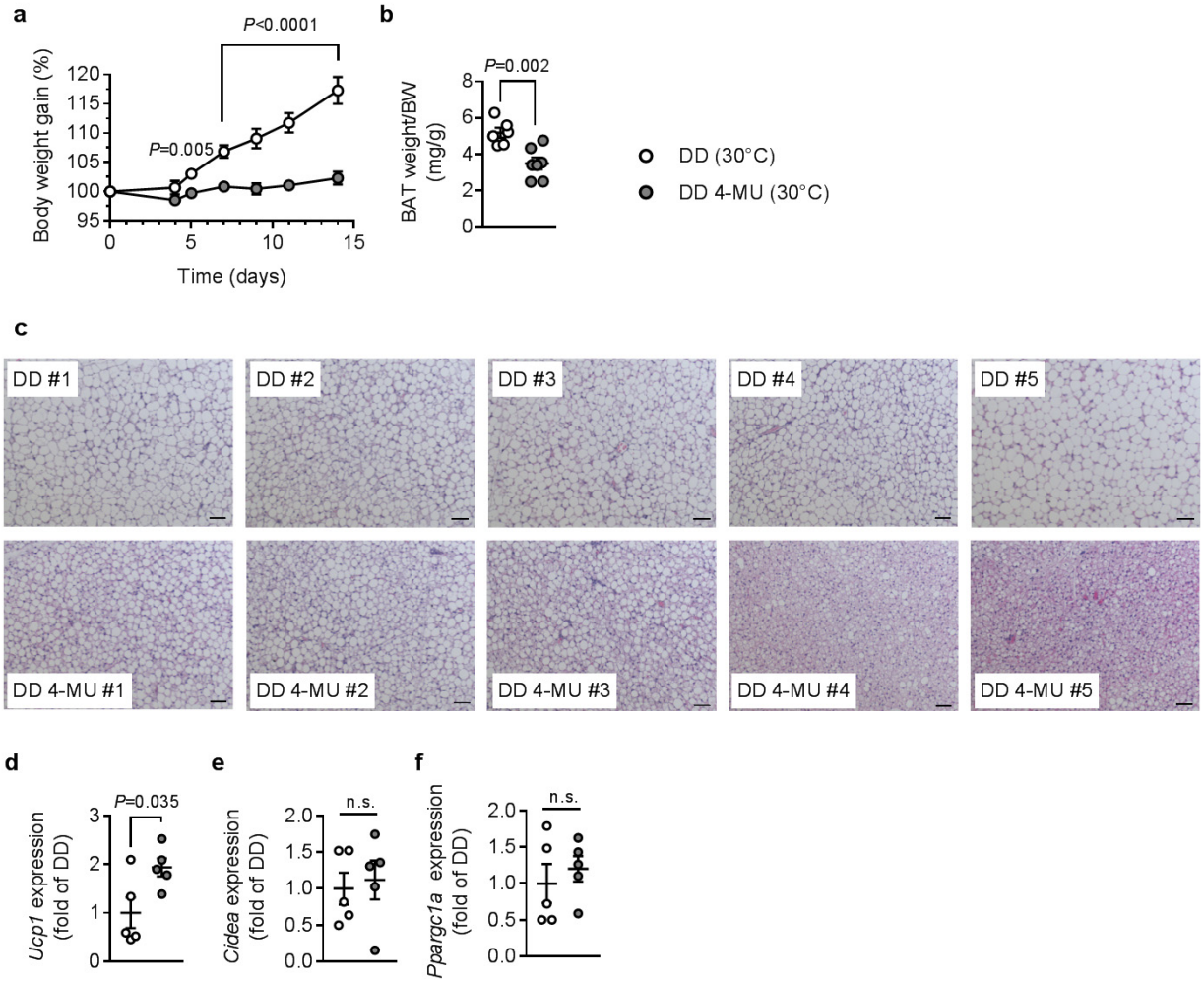

Supplementary Figure 7 4-MU reduces body weight and increases *Ucp1* expression at thermoneutrality. After 4 weeks of adaptation at 30°C, C57BL6/J mice were fed either diabetogenic diet (DD) alone or DD supplemented with 4-MU (DD 4-MU) for two weeks. Body weight gain (**a**; n = 5,5 mice), brown adipose tissue (BAT) weight normalized to body weight; $P < 0.0001$versus DD (**b;** n = 6,7 biologically independent samples) as well as representative images of adipose tissue (**c**) from 5 mice fed with DD and DD 4-MU, respectively, are shown. Scale bars indicate 50 µm. mRNA expression of *Ucp1, Cidea,* and *Ppargc1a* in 4-MU treated mice (**d-f**; n = 5,5 biologically independent samples). Data are presented as means ± s.e.m.. (**a**) Two-way ANOVA with post hoc Sidak's multiple comparison test, (**b, d, f**) two-tailed unpaired Student's *t*-test or (**e**) Mann-Whitney test. n.s.: not significant.

Supplementary Figure 8

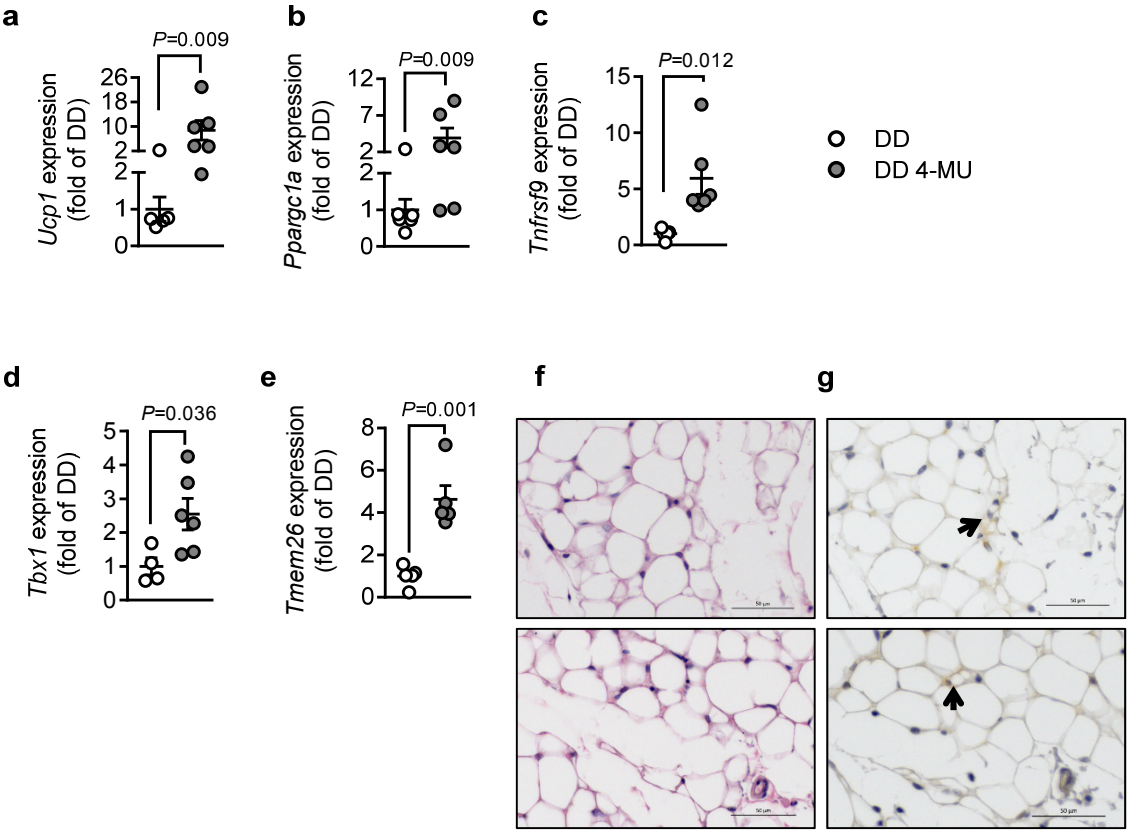

Supplementary Figure 8 4-MU induces beiging markers in inguinal adipose tissue after 22 weeks of treatment. mRNA expression of multiple beiging markers such as (**a**) *Ucp1,* n = 5,6 biologically independent samples; (**b**) *Ppargc1a*, n = 6,6 biologically independent samples; (**c**) *Tnfrsf9,* n = 5,6 biologically independent samples; (**d**) *Tbx1,* n = 4,6 biologically independent samples; (**e**) *Tmem26,* n = 5,5 biologically independent samples in inguinal adipose tissue from mice treated for 22 weeks with diabetogenic diet (DD) or DD supplemented with 4-MU (DD 4-MU). Inguinal adipose tissue of DD 4-MU treated mice was harvested, fixed, and embedded for paraffin sections followed by (**f**) HE staining and (**g**) staining of UCP1. Two representative pictures of browning from n=4 biological samples are shown; arrows indicate UCP1-positive stained cells. Scale bars indicate 50 µm. Data are presented as means ± s.e.m.. (**a**, **b**) Two-tailed Mann-Whitney test**, (c**-**e**) two-tailed unpaired Student's *t*-test.

Supplementary Figure 9

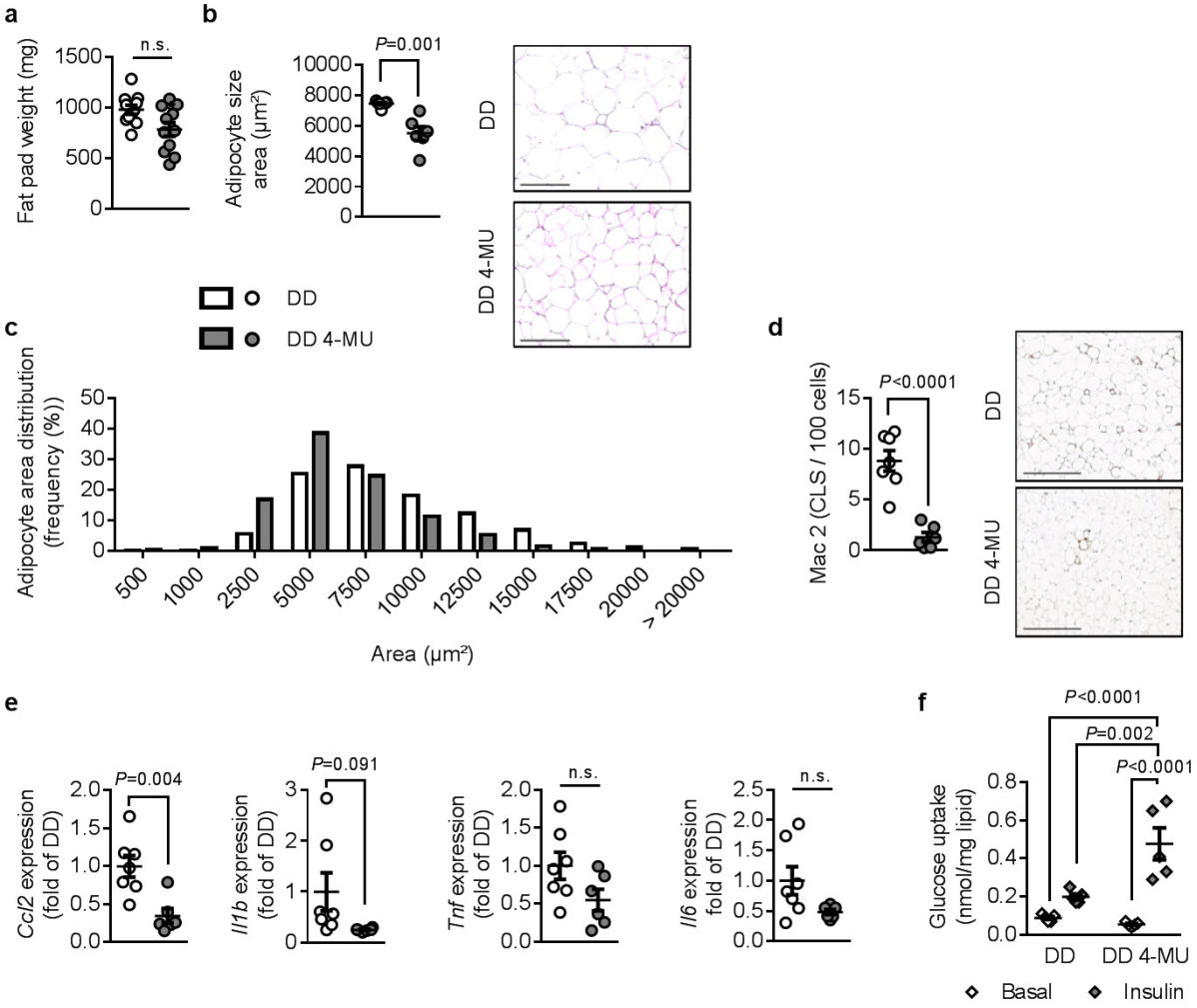

Supplementary Figure 9 4-MU reduces adipocyte hypertrophy and inflammation and improves glucose uptake in white adipose tissue. (**a**) Weight of epididymal adipose tissue (AT) after 22 weeks of feeding male C57BL/6J mice diabetogenic diet without (DD) or with 4-MU (DD 4-MU), n = 11,11 biologically independent samples. (**b**) Analysis of white adipocyte area in epididymal AT after 22 weeks of feeding, n = 7,6 biologically independent samples. Representative images from H&E staining are shown; scale bars indicate 200 µm. (**c**) Cell size distribution in epididymal AT of C57BL/6J mice after 22 weeks of feeding, n = 11,11 biologically independent samples. (**d**) Quantification (number of crown-like structures (CLS) per 100 cells) and representative images of Mac2 staining in epididymal AT after 22 weeks of feeding, n = 7,6 biologically independent samples; scale bars indicate 500 µm. (**e**) mRNA expression of inflammatory genes *Ccl2, Il1b, Tnf,* and *Il6* in epididymal AT after 22 weeks of feeding as analyzed by qPCR, n = 7,6 biologically independent samples. (**f**) *Ex vivo* measurement of basal and insulin-dependent glucose uptake in isolated adipose cells from epididymal AT after 16 weeks of feeding, n = 5,5 biologically independent samples. Data are presented as means ± s.e.m.. (**a, b, d, e**) Two-tailed unpaired Student's *t*-test, except for *Il1b* and *Il6* expression: Mann-Whitney test and (**f**) two-way ANOVA with Sidak's multiple comparison test. n.s.: not significant.

Supplementary Figure 10

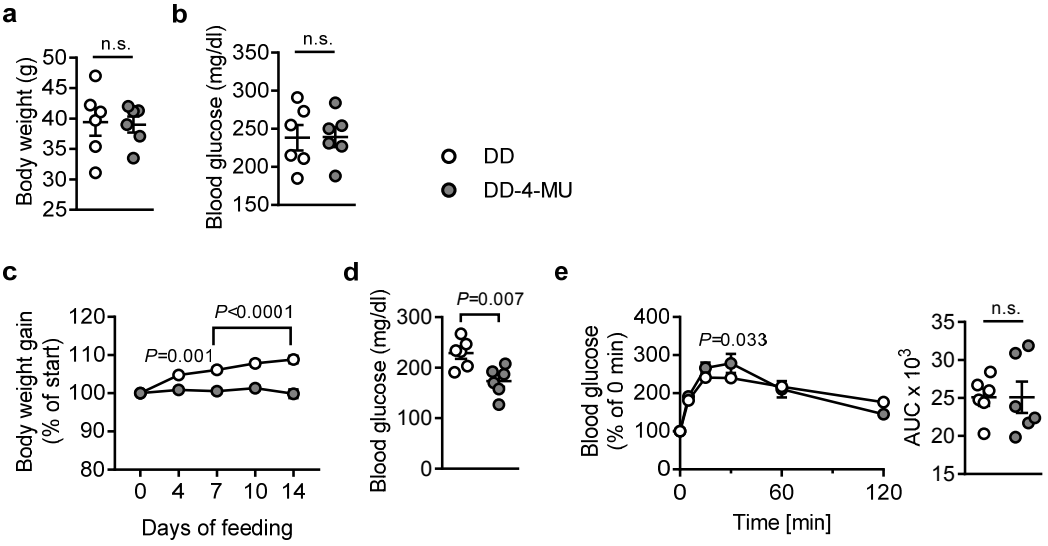

Supplementary Figure 10 4-MU reduces body weight gain and improves glucose homeostasis in mice with established insulin resistance. After 8 weeks of feeding DD, male obese and insulin-resistant C57BL6/J mice were randomized to either a group receiving diabetogenic diet (DD) or a group receiving DD supplemented with 4-MU (DD 4-MU). (**a**) Body weight, n = 6,6 mice, and (**b**) blood glucose, n = 6,6 biologically independent samples, of mice 8 weeks after being randomized to the two aforementioned treatment groups. (**c**) Body weight gain and (**d**) fasting blood glucose as well as (**e**) ipGTT (blood glucose depicted as % of baseline) and respective AUC after 2 weeks on DD or DD 4-MU. (**a-e**) n = 6,6 mice/biologically independent samples. Data are presented as means ± s.e.m.. (**c, e** left) Two-way ANOVA with post hoc Sidak`s multiple comparison test (*P* versus DD) or (**a, b, d**, **e** right) two-tailed unpaired Student's *t*-test. n.s.: not significant.

Supplementary Figure 11

a

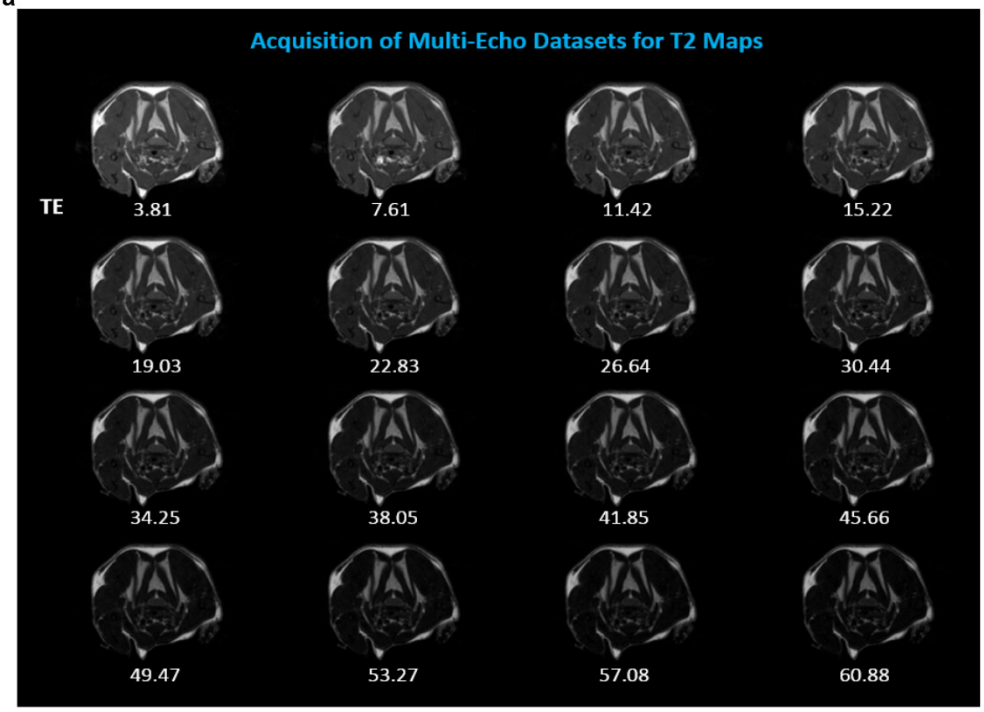

b

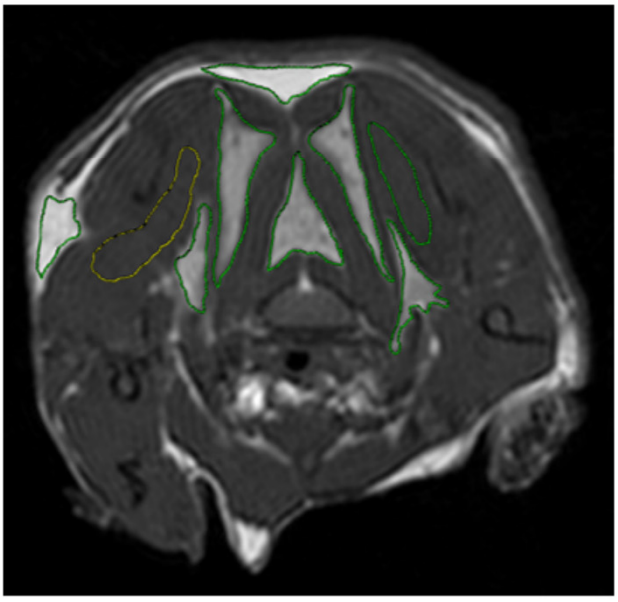

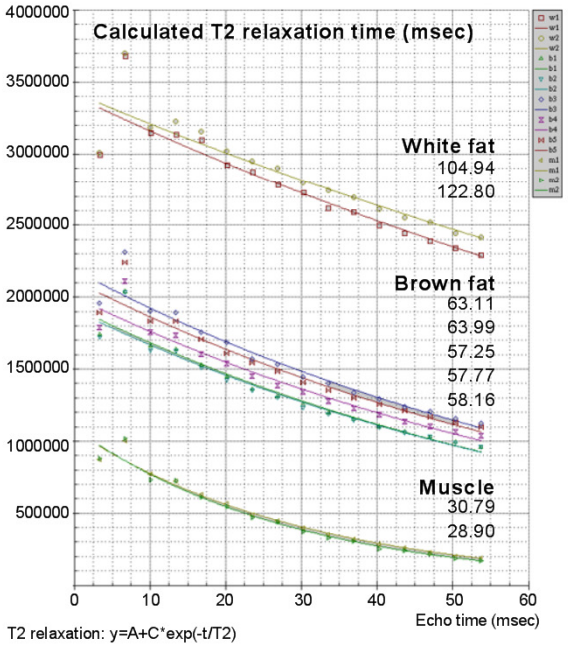

Supplementary Figure 11 T2 map generation and quantification. (**a**) Representative magnetic resonance (MR) images from a train of 16 echoes covering the dorsocervical brown adipose tissue (BAT). An exponential curve was fitted to the intensity decay of each pixel in order to generate the T2 maps. (**b**) Demarcations for white and brown adipose tissue as well as muscle were manually drawn (green) with the ParaVision Region-of-Interest (ROI) tool (left) and tissue-specific T2 times were determined from the respective ROIs (right). For each slice, 2 separated ROIs were evaluated for white adipose tissue (WAT) and muscle, respectively, while for BAT as many ROIs were used as required for complete coverage of all tissue parts. T2 values for BAT, WAT, and muscle were then averaged over all ROIs from all slices. (**a, b**) 4 independently repeated experiments.

Supplementary Figure 12

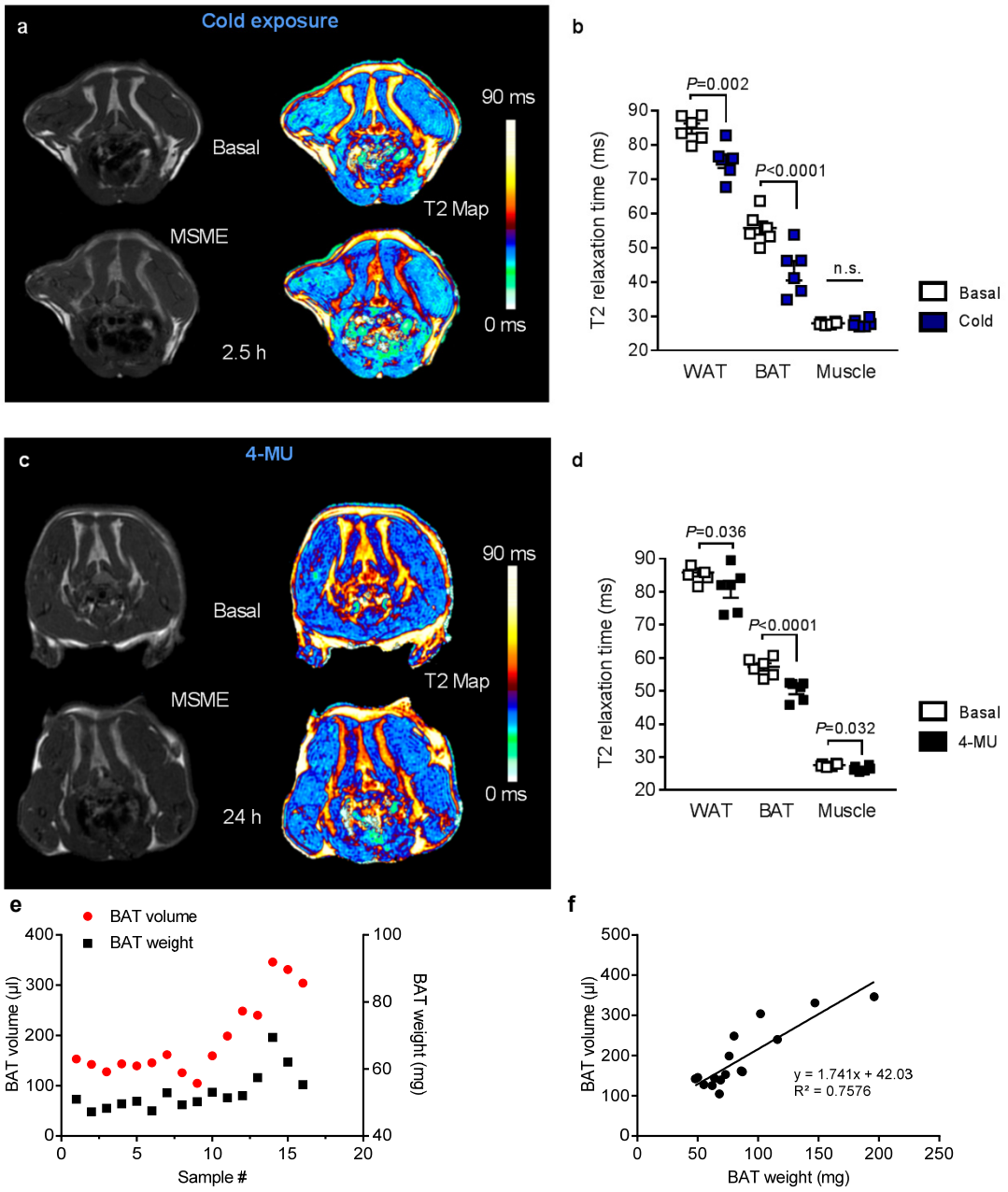

Supplementary Figure 12 T2 Mapping of cold exposure and 4-MU treatment.
(**a**) Selected images from a multi-slice multi-echo (MSME) magnetic resonance (MR) dataset (left) and corresponding T2 maps with color coding from 0 ms to 90 ms (right) recorded from the same animal before (top) and after 2.5 h of cold (4°C) exposure (bottom). Brown adipose tissue (BAT) activation is indicated by a color change in the T2 maps from yellow to red (right top and bottom). (**b**) Quantification of T2 values for white adipose tissue (WAT), BAT, and muscle before and after 2.5 h of cold exposure with a drop in BAT T2 similar to the CL-316 stimulation shown in Figure 4 (n = 6,6 mice). (**c**) Representative MSME MR images (left) and T2 maps (right) acquired from the dorsocervical BAT of the same animal before (top) and after 24 h of 4-MU administration (bottom). In the color-coded T2 maps (0 to 90 ms), BAT activation is again reflected by a change from yellow to red (right top and bottom). (**d**) Quantification of T2 values for WAT, BAT, and muscle before and after 24 h of 4-MU administration (n = 6,6 mice). Total BAT weight was measured directly after MRI measurements and organ weights were compared to the calculated BAT volume based on planimetry of T2 maps. (**e**) Absolute values of BAT volume and weight in 16 individual samples from independent measurements. (**f**) Correlation of BAT weight and volume, linear regression, n = 16 biologically independent samples. Data are presented as means ± s.e.m.. (**b, d**) Two-tailed paired Student's *t*-test. (**a, c**) 3 independently repeated experiments. n.s.: not significant.

Supplementary Figure 13

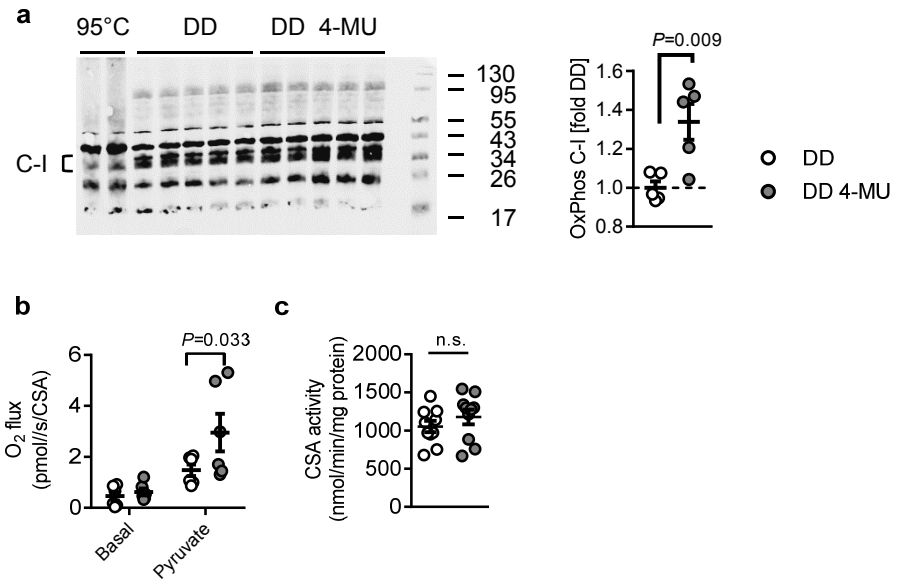

Supplementary Figure 13 Long-term 4-MU treatment increases mitochondrial complex I and respiration in brown adipose tissue (BAT). (**a**) Determination of mitochondrial complex I (C-I) protein expression in BAT (left: western blot, right: respective quantification), n = 5,5 biologically independent samples. Samples boiled at 95°C were used as a control for heat-degradable C-I. (**b**) Mitochondrial respiratory capacity of BAT under basal and pyruvate (complex I)-stimulated conditions (n = 6,6 biologically independent samples) and (**c**) citrate synthase activity (CSA) in BAT as a marker of mitochondrial density (n = 10,10 biologically independent samples) after 22 weeks of feeding mice with diabetogenic diet (DD) or DD supplemented with 4-MU, respectively. Data are presented as means ± s.e.m.. (**a, c**) Two-tailed unpaired Student's *t*-test; (**b**) two-way ANOVA with Sidak`s multiple comparisons tests. n.s.: not significant.

Supplementary Figure 14

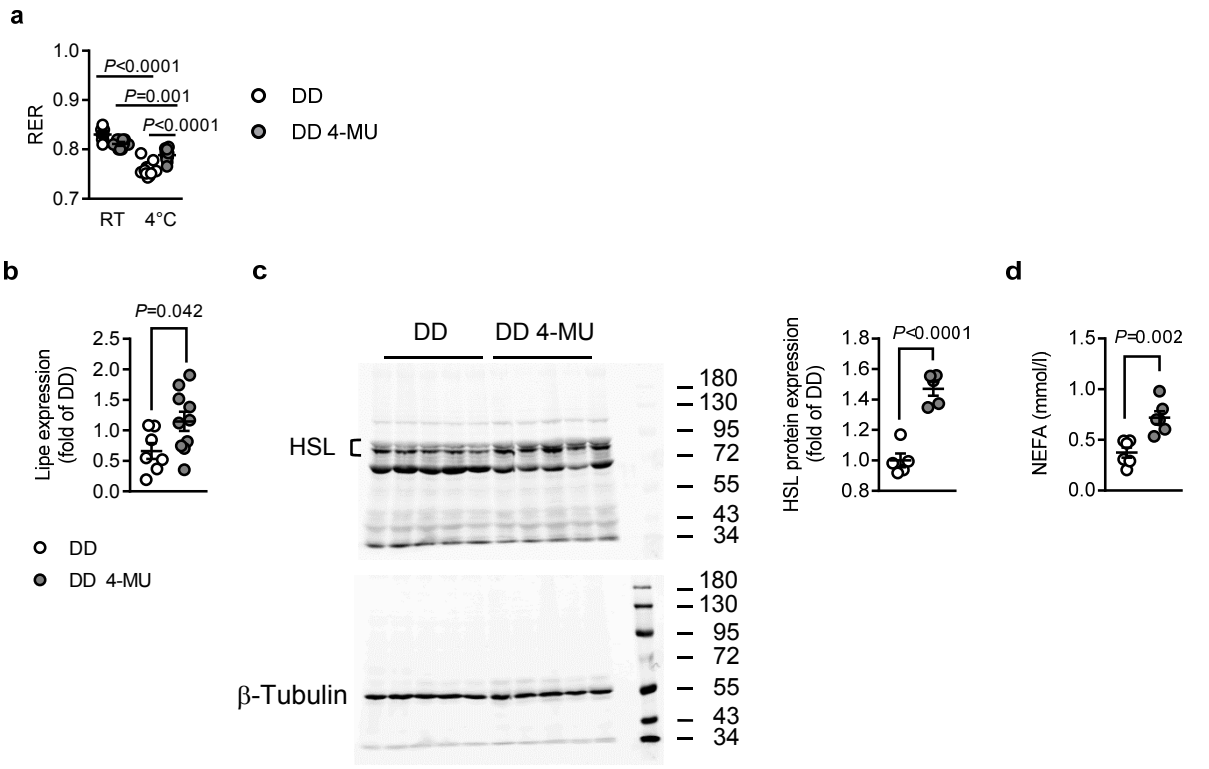

Supplementary Figure 14 4-MU shifts the respiratory exchange ratio and increases expression of hormone-sensitive lipase (HSL). (**a**) The respiratory exchange ratio (RER) during measurement of basal energy expenditure at 21°C (n = 8,10 mice) and during 8 hours of cold exposure (4°C; n = 12,10 mice). After 11 weeks of feeding diabetogenic diet (DD) or DD supplemented with 4-MU (DD 4-MU), brown adipose tissue (BAT) was analyzed for expression of hormone-sensitive lipase (HSL) on (**b**) mRNA level (n = 7,10 biologically independent samples) or (**c**) protein level (n = 5,5 biologically independent samples). (**d**) Non-esterified free fatty acids (NEFA) were measured in plasma from fasted mice (n = 6,6 biologically independent samples). Data are presented as means ± s.e.m. (**a**) One-way ANOVA with Bonferroni's multiple comparisons test, (**b-d**) two-tailed unpaired Student's *t*-test.

Supplementary Figure 15

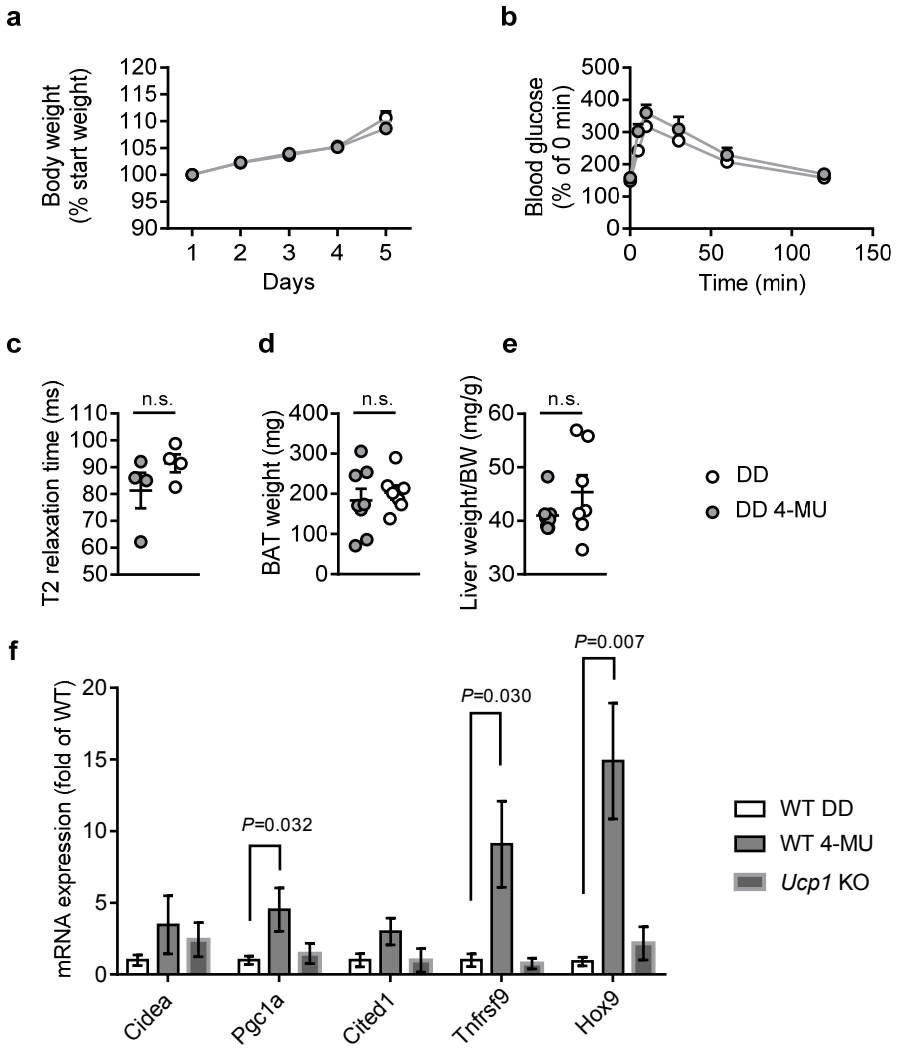

Supplementary Figure 15 Lack of *Ucp1* abolishes 4-MU-mediated beneficial effects on the metabolic phenotype. Male, 20-week-old *Ucp1* knock out (KO) mice were fed a diabetogenic diet (DD) supplemented without or with 4-MU (DD 4-MU). (**a**) Mice were pair-fed for 5 days and body weight gain was assessed every day; n = 7,8 mice. (**b**) A glucose tolerance test (GTT) was performed after 4 weeks of feeding DD or DD 4-MU; n = 7,8 biologically independent samples. (**c**) After 8 weeks of feeding either DD or DD 4-MU, T2 relaxation time of brown adipose tissue (BAT) was assessed by magnetic resonance imaging (MRI); n = 4 biologically independent samples. Organ weights of (**d**) BAT and (**e**) liver after 8 weeks of feeding DD or DD 4-MU (n = 8,7 biologically independent samples). **(f)** Inguinal adipose tissue from age-matched C57BL/6J wildtype (WT) or *Ucp1* KO mice fed with DD or DD 4-MU under thermoneutral conditions was compared regarding mRNA expression of beiging markers such as *Cidea* (n=6,6,4 biologically independent samples), *Pgc1a* (n=6,6,4 biologically independent samples), *Cited1* (n=5,6,3 biologically independent samples), *Tnfrsf9* (n=5,6,4 biologically independent samples), and *Hox9* (n=6,5,4 biologically independent samples). Data are presented as mean ± s.e.m. (**a, b**) Two-way ANOVA with Sidak's multiple comparison test, (**c-e**) two-tailed unpaired Student's *t*-test or (**f**) One-way ANOVA with Dunnett`s multiple comparisons test . n.s.: not significant.

Supplementary Figure 16

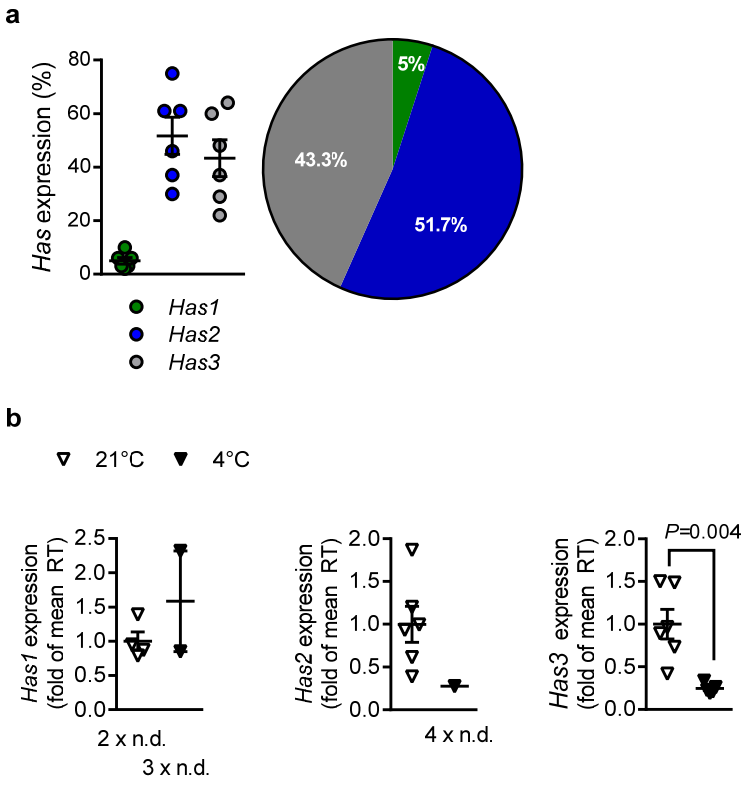

Supplementary Figure 16 Feeding diabetogenic diet and cold exposure strongly regulate the HA system. (**a**) Basal mRNA expression profile of HA synthases in brown adipose tissue (BAT); n = 6,6 biologically independent samples. (**b**) Male, 8-week-old C57BL/6J mice were kept at 21°C exposed to cold for 8 hours followed by immediate harvest of BAT tissue. mRNA expression of *Has1* (n = 4,2 biologically independent samples) ,-2 (n = 6,1 biologically independent samples), *and -3* (n = 6,5 biologically independent samples) were detected by qPCR. Data are presented as means ± s.e.m.. (**b**) Two-tailed unpaired Student's *t*-test. n.d. not detectable.

Supplementary Figure 17

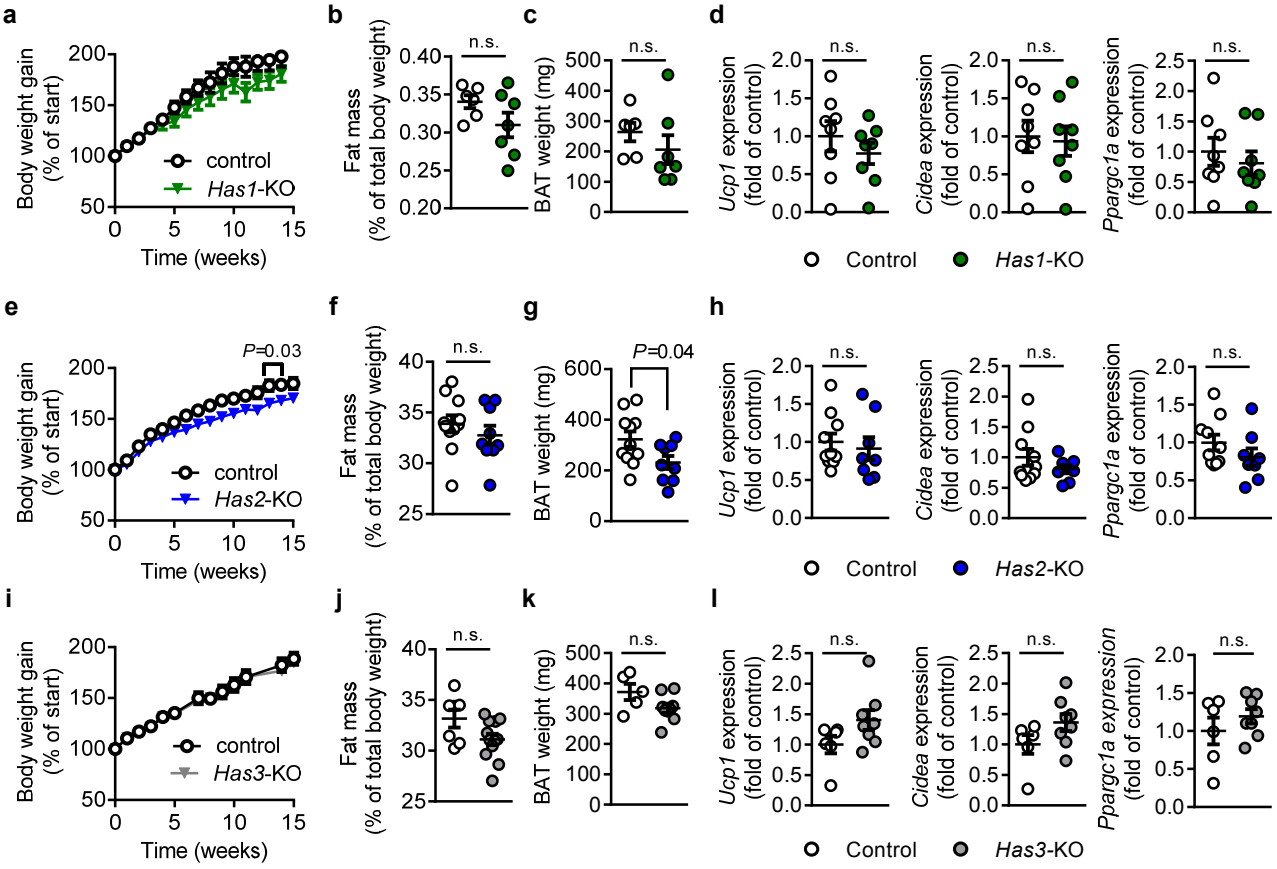

Supplementary Figure 17 Body weight gain and brown adipose tissue (BAT) activation in *Has*-deficient mice.
(**a**) Body weight gain in *Has1*-deficient mice after start of feeding diabetogenic diet (DD); n = 7,7. (**b**) Total body fat content of *Has1*-deficient mice after 17 weeks of feeding DD; n = 6,7. (**c**) BAT weight from *Has1*-deficient vs. wildtype control mice after 22 weeks of feeding; n = 6,7 biologically independent samples. (**d**) *Ucp1*, *Cidea*, and *Ppargc1a* mRNA in BAT from *Has1*-deficient vs. wildtype control mice as determined by qPCR; n = 6,8 biologically independent samples. (**e**) Body weight of *Has2*-deficient mice after start of feeding; n = 11,9. (**f**) Total body fat content of *Has2*-deficient mice after 17 weeks of feeding; n = 11,9 biologically independent samples. (**g**) BAT weight from *Has2*-deficient vs. respective control mice after 22 weeks of feeding; n = 11,9 biologically independent samples. (**h**) *Ucp1*, *Cidea*, and *Ppargc1a* mRNA in BAT of *Has2*-deficient vs. respective control mice as determined by qPCR; n = 10,8 biologically independent samples. (**i**) Body weight gain of *Has3*-deficient mice after start of feeding; n = 6,8. (**j**) Total body fat content of *Has3*-deficient mice after 17 weeks of feeding; n = 7,12 . (**k**) BAT weight from *Has3*-deficient vs. wildtype control mice after 22 weeks of feeding; n = 4,5. (**l**) *Ucp1*, *Cidea*, and *Ppargc1a* mRNA in BAT of *Has3*-deficient vs. wildtype control mice as determined by qPCR, n = 6,8 biologically independent samples. Data are presented as means ± s.e.m., (**a,e,i**) Two-way ANOVA with Sidak's multiple comparison test (*P* versus control) or (**b-d,f-h,j-l**) two-tailed unpaired Student's *t*-test. n.s.: not significant.

Supplementary Figure 18

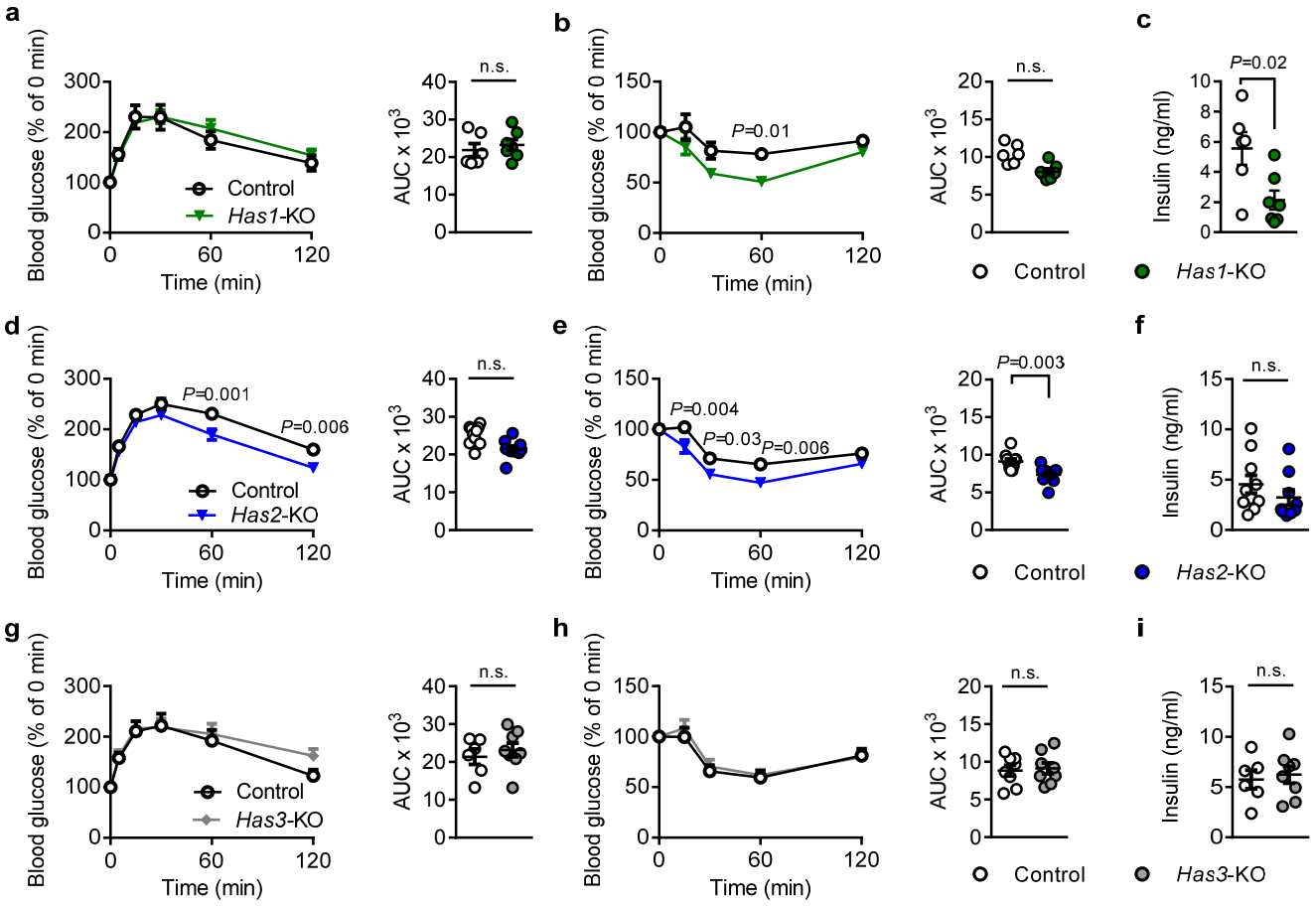

Supplementary Figure 18 Glucose homeostasis in *Has*-deficient mice.
(**a**) Intraperitoneal glucose tolerance test (ipGTT) performed in *Has1*-deficient mice after 19 weeks of feeding diabetogenic diet (DD), n = 10,9. (**b**) Insulin tolerance test (ITT) performed in *Has1*-deficient mice after 20 weeks of feeding DD, n = 6,7. (**c**) Fasting plasma insulin concentration in *Has1*-deficient mice after 22 weeks of feeding DD, n = 6,7 biologically independent samples. (**d**) ipGTT performed in *Has2*-deficient mice after 19 weeks of feeding DD, n = 10,9. (**e**) ITT performed in *Has2*-deficient mice after 20 weeks of feeding DD, n = 10,9. (**f**) Fasting plasma insulin concentration after 22 weeks of feeding DD, n = 10,9. (**g**) ipGTT performed in *Has3*-deficient mice after 19 weeks of feeding DD, n = 6,8 biologically independent samples. (**h**) ITT performed in *Has3*-deficient mice after 20 weeks of feeding DD, n = 8. (**i**) Fasting plasma insulin concentration after 22 weeks of feeding DD, n = 6,8 biologically independent samples. For all tolerance tests, blood glucose concentration depicted as % of 0 minutes (left) and respective area under the curve (AUC; right) are shown. Data are presented as means ± s.e.m. (**a** left, **b** left, **d** left, **e** left, **g** left, **h** left) Two-way ANOVA with post hoc Sidak's multiple comparison test (*P* versus control) or (**a** right, **b** right, **c,** **d** right, **e** right, **f**, **g** right, **h** right, **i**) two-tailed unpaired Student's *t*-test. n.s.: not significant.

Supplementary Figure 19

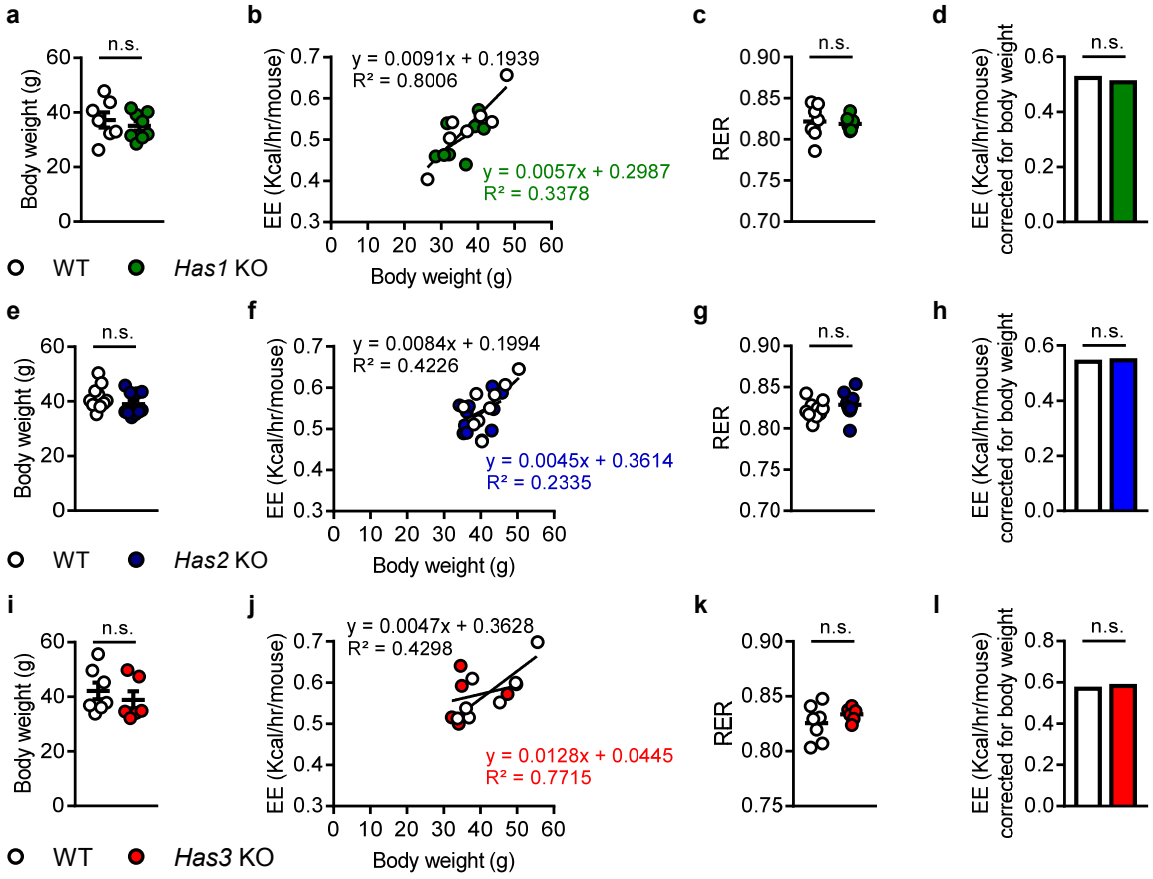

Supplementary Figure 19 Energy expenditure (EE) of *Has*-deficient mice. Analysis of energy expenditure of *Has1*- *Has2*- and *Has3*-deficient mice and respective control mice after 11 weeks of feeding diabetogenic diet (DD). Analysis of *Has1* deficient and control mice showing (**a**) body weight (**b**) body weight against raw energy expenditure (**c**) RER (**d**) Energy expenditure corrected for body weight using ANCOVA. Covariates assessed at BW =36.1 g. Analysis of *Has2*-deficient and control mice showing (**e**) body weight (**f**) body weight against raw energy expenditure (**g**) RER (**h**) Energy expenditure corrected for body weight using ANCOVA. Covariates assessed at BW = 40.3 g. Analysis of *Has3*-deficient and control mice showing (**i**) body weight (**j**) body weight against raw energy expenditure (**k**) RER (**l**) Energy expenditure corrected for body weight using ANCOVA. Covariates assessed at BW =41.7 g. (**a**) n = 7,8 mice, (**b**) n = 10,10 mice and (**c**) n = 4,6 mice. (**b**, **f**, **j**) Linear regression. Data are presented as means ± s.e.m.. n.s.: not significant.

Supplementary Figure 20

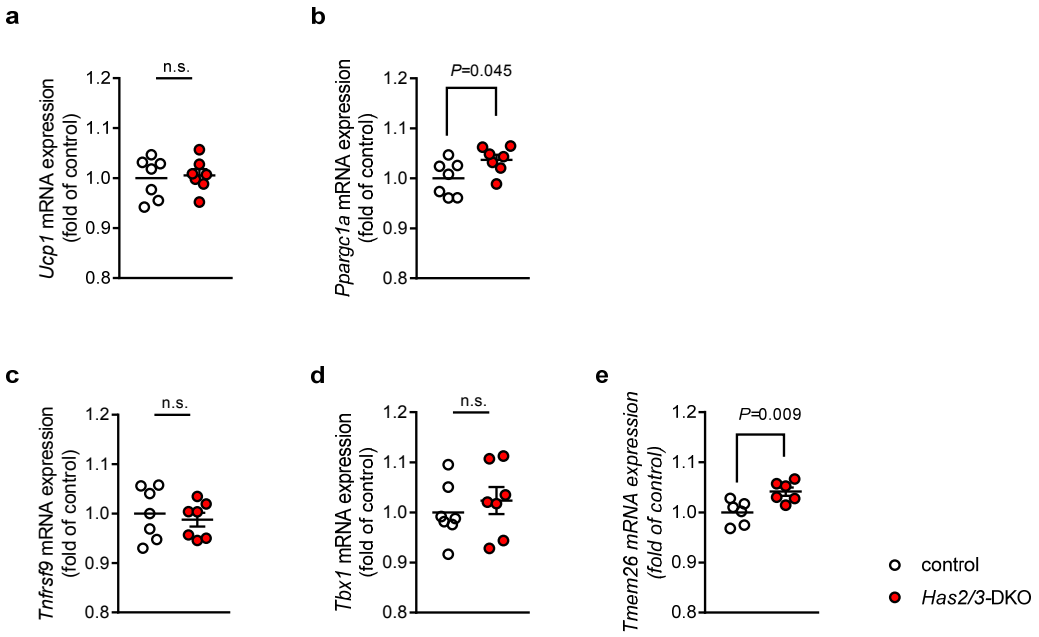

Supplementary Figure 20 *Has2/3*-double deficient mice show trends towards increased beiging of inguinal adipose tissue. mRNA expression of multiple beiging markers was analyzed by qPCR in inguinal adipose tissue from *Has2/3*-double deficient mice (*Has2/3*-DKO) or respective control mice after start of feeding diabetogenic diet (DD) for 11 weeks (**a-d**); n = 7,7 biologically independent samples; (**e**); n = 6,7 biologically independent samples. Data are presented as means ± s.e.m.; two-tailed unpaired Student's *t*-test. n.s.: not significant.

TABLE 1

Murine primer sequences:

GEN	*FORWARD* PRIMER 5'-3'	*REVERSE* PRIMER 5'-3'
18S rRNA	GCAATTATTCCCCATGAACG	GGCCTCACTAAACCATCCAA
Cidea	GCAGCCTGCAGGAACTTATC	TCATGAAATGCGTGTTGTCC
Has1	TATGCTACCAAGTATACCTCG	TCTCGGAAGTAAGATTTGGAC
Has2	CAAAAATGGGGTGGAAAGAG	ACAGATGAGGCAGGGTCAAG
Has3	CTCAGTGGACTACATCCAGG	GACATCTCCTCCAACACCTC
Il1β	GGATGAGGACATGAGCACCT	CGTCACACACCAGCAGGTTA
Il6	GATGGATGCTACCAAACTGGA	GGTACTCCAGAAGACCAGAGGA
Mcp1	TTCCTTCTTGGGGTCAGCAC	GGCTGGAGAGCTACAAGAGG
Lipe	GGGCTTCCAGTTCACACCTG	GAATCGGCCACCGGTAAAGA
Pgc1α	GCGGACAGAATTGAGAGACC	CATTCTCAAGAGCAGCGAAA
Tnfα	TCGAGTGACAAGCCTGTAGC	AAGGTACAACCCATCGGCTG
Ucp1	TCAGGATTGGCCTCTACGAC	TGCCACACCTCCAGTCATTA
Vegfα	AGCTTCCTACAGCACAGCAG	TGAGAGGTCTGGTTCCCGAA
Slc2a4	ATCATCCGGAACCTGGAGG	CGGTCAGGCGCTTTAGACTC
Gpi1	ATGGGCATATTCTGGTGGAC	CCCGATTCTCGGTGTAGTTG
Pfkl	GCCTATCTCATCCAGCTACG	CTTGCTACTCAGGATTCGGT
Pfkp	AAGCTATCGGTGTCCTGACC	TCCCACCCACTTGCAGAAT
Pgk1	GAGCCTCACTGTCCAAACTA	CTTTAGCGCCTCCCAAGATA
Hk2	AGAGAACAAGGGCGAGGAG	GGAAGCGGACATCACAATC

GEN	Qiagen Quantitect Primer Assay
Tnfrsf9	Mm_Tnfrsf9_1_SG (Cat. No.: QT00147266)
Tbx1	Mm_Tbx1_1_SG (Cat. No.: QT00158627)
Tmem26	Mm_Tmem26_1_SG (Cat. No.: QT00125055)

TABLE 2

Human primer sequences:

GEN	*FORWARD* PRIMER 5'-3'	*REVERSE* PRIMER 5'-3'
18S	GCAATTATTCCCCATGAACG	GGCCTCACTAAACCATCCAA
UCP-1	TCTCTCAGGATCGGCCTCTA	GCCCAATGAATACTGCCACT
CIDEA	AGACCTTGGGAGACAACACG	ACTCTCGCTATTCCCGACCT
PPARGC1A	GCCCAGGTATGACAGCTACG	CTGTCCGTGTTGTGTCAGGT